Pergamon

0301-9322(94)00064-6

Int. J. Multiphase Flow Vol. 21, No. 3, pp. 515–528, 1995

0301-9322/95 $9.50 + 0.00

PULSATILE FLOW AND HEAT TRANSFER OF A DUSTY FLUID THROUGH AN INFINITELY LONG ANNULAR PIPE

N. DATTA and D. C. DALAL†

Department of Mathematics, Indian Institute of Technology, Kharagpur-721 302, India

(Received 9 April 1993; in revised form 15 July 1994)

Abstract—The flow and heat transfer of a dusty fluid within the annulus of circular cylinders under a pulsatile pressure gradient has been studied. Using Saffman's model for the dusty fluid the problem has been solved analytically and results discussed with the help of graphs. It is observed that the velocity of the fluid as well as that of the particle phase decreases with decrease of annular gap and increases with decrease of frequency of oscillation. The rate of heat transfer of fluid at the outer wall decreases with decrease of annular gap but the effect is opposite at the inner wall. The heat transfer rate increases with decrease of frequency of oscillation at both walls and the effect of volume fraction of dust particles is appreciable at large values of frequency of oscillation.

Key Words: pulsatile flow, dusty fluid, heat transfer, volume fraction, amplitude, phase lag, frequency parameter, aspect ratio

1. INTRODUCTION

The study of heat transfer to a single-phase fluid flow through an annular tube has been made by several authors because of its application in a variety of heat transfer systems ranging from simple heat exchangers to most complicated nuclear reactors. Jakob & Rees (1941) made a theoretical investigation of the problem of heat transfer through the annular space when the fluid flow is laminar and there is uniform heating either from outside, from inside or from both. Reynolds *et al.* (1960), McCuen *et al.* (1961, 1962), Leung *et al.* (1962) and Heaton *et al.* (1962) of Stanford University have made numerous theoretical and experimental studies of both laminar and turbulent heat transfer in annuli taking various types of wall temperature distributions. Reynolds *et al.* (1962) have also included a bibliography of the related work on this aspect. Shigechi *et al.* (1991) have made an analysis on laminar flow and heat transfer in concentric annuli with moving cores to obtain the effect of relative velocity on friction factor and Nusselt number.

Uchida (1956) has investigated the pulsating flow superposed on a steady flow of a viscous clear fluid in a circular pipe. The problem of heat transfer in a pulsatile flow of an elastico-viscous fluid in a porous parallel plate channel has been solved by Soundalgakar *et al.* (1989).

The study of flow and heat transfer of a dusty fluid through annular pipes has wide applications in many industries. This helps in the design of chemical reactors where the flow is creeping and heat transfer is not large. Available literature does not contain many analytical studies on this problem.

A technical review of experimental and theoretical studies of heat transfer to a flowing gas–solid mixture has been presented by Depew & Kramer (1973). Turbulent heat transfer characteristics of gas–particle flow in a pipe have been studied by Michaelides (1986) and Han *et al.* (1991). Singh (1973) has studied the flow of a dusty gas through circular annuli.

The present work is on the fully developed laminar flow and heat transfer of a dusty fluid in an infinite annular pipe with a pulsatile pressure gradient.

2. MATHEMATICAL FORMULATION

Certain simplifying assumptions are usually made to study dusty fluid flows (Saffman 1962; Marble 1962). Dust particles are assumed to be spherical in shape and of equal size and mass.

†Present address: Physics and Applied Mathematics Unit, Indian Statistical Institute, 203 B.T. Road, Calcutta-700 035, India.

We also assume the bulk concentration of the dust to be very small and the Reynolds number, based on the relative motion of the dust particles and fluid, to be small compared to unity, as a result, the net effect of the dust particles on the fluid is equivalent to an extra force given by Stokes drag. Other forces of interaction (i.e. gravity, Basset etc.) have been neglected. The volume fraction of the particles has been assumed to be small so that particle–particle interaction is negligible but large enough for the particle phase to form a pseudo-fluid. The dusty fluid flow can then be assumed to be a two-phase fluid flow. Due to lack of randomness in local particle motion, pressure associated with the particle cloud is negligible. The viscosity of the particle phase is also negligible.

Under these assumptions, the governing equations for laminar flow and heat transfer of the two phases can be written as:

For the fluid phase:

$$\frac{\partial}{\partial t}\{\rho(1-\phi)\} + \operatorname{div}\{\rho(1-\phi)\mathbf{q}\} = 0 \qquad [1]$$

$$(1-\phi)\rho\left\{\frac{\partial \mathbf{q}}{\partial t} + (\mathbf{q}\cdot\nabla)\mathbf{q}\right\} = -\nabla p + \nabla(\mu\nabla\cdot\mathbf{q}) + \mathbf{F}_p, \qquad [2]$$

$$(1-\phi)\rho c_p\left\{\frac{\partial T}{\partial t} + (\mathbf{q}\cdot\nabla)T\right\} = \frac{\partial p}{\partial t} + (\mathbf{q}\cdot\nabla)p + q_f + Q_p + (\mathbf{q}_p - \mathbf{q})\cdot\mathbf{F}_p + \Phi, \qquad [3]$$

For the particle phase:

$$\frac{\partial \rho_p}{\partial t} + \operatorname{div}(\rho_p \mathbf{q}_p) = 0, \qquad [4]$$

$$\rho_p\left\{\frac{\partial \mathbf{q}_p}{\partial t} + (\mathbf{q}_p\cdot\nabla)\mathbf{q}_p\right\} = -\mathbf{F}_p, \qquad [5]$$

$$\rho_p c_s\left\{\frac{\partial T_p}{\partial t} + (\mathbf{q}_p\cdot\nabla)T_p\right\} = -Q_p \qquad [6]$$

where $\rho_p = Nm = \phi\rho_s$ is the density of the particle phase; $\mathbf{F}_p = \rho_p(\mathbf{q}_p - \mathbf{q})/\tau_p$ is the velocity interaction force between the fluid and the particle phase; $q_f = \nabla\cdot(k\nabla T)$ is the rate of heat added to the fluid by conduction in unit volume; $Q_p = \rho_p c_s(T_p - T)/\tau_T$ is the thermal interaction between the fluid and the particle phase; Φ is the viscous dissipation of the fluid; $\mathbf{q}, \rho, \mathrm{p}, \mu, T, c_p, k$ are, respectively, the velocity vector, density, pressure, coefficient of viscosity, temperature, specific heat and thermal conductivity of the fluid $\mathbf{q}_p$, T_p, ρ_s, N, m, c_s, ϕ, τ_p and τ_T are, respectively, the velocity vector, temperature, material density, number density, mass, specific heat, volume fraction, velocity relaxation time and thermal relaxation time of particles; and t is time.

The pulsatile flow and heat transfer of a dusty fluid through an annulus bounded by two infinitely long co-axial circular cylinders in which a and b are the radii of the outer and inner cylinders, respectively, has been considered. Taking the z-axis along the common axis of the cylinders (figure 1), the outer and inner walls are given by $r = a$ and $r = b$, respectively.

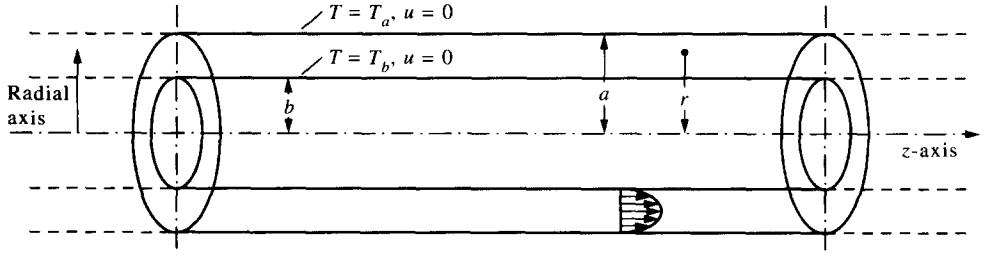

Figure 1. Schematic diagram of an annular pipe.

Considering the flow to be fully developed and symmetric, the velocity and temperature are functions of the radial distance r and time t only. Here, the flow is assumed to be unidirectional. So, the continuity equation of the fluid and the particle phase will be automatically satisfied. We also consider the number density of the particles N to be constant, N_0, because flow is incompressible and no mass transfer is considered. The study is confined to flows at low Reynolds number and with a moderate variation of temperature so that the viscosity of the fluid may be taken as constant.

The governing equations of momentum and energy from [1]–[6] can be written, in cylindrical co-ordinates, as (Singleton 1965):

For the fluid phase:

$$\rho(1-\phi)\frac{\partial u}{\partial t} = -\frac{\partial p}{\partial z} + \mu\left\{\frac{\partial^2 u}{\partial r^2} + \frac{1}{r}\frac{\partial u}{\partial r}\right\} + \frac{\rho_p}{\tau_p}(u_p - u), \tag{7}$$

$$\rho c_p(1-\phi)\frac{\partial T}{\partial t} = k\left\{\frac{\partial^2 T}{\partial r^2} + \frac{1}{r}\frac{\partial T}{\partial r}\right\} + \mu\left(\frac{\partial u}{\partial r}\right)^2 + \frac{\rho_p}{\tau_p}(u_p - u)^2 + \frac{\rho_p c_s}{\tau_T}(T_p - T), \tag{8}$$

For the particle phase:

$$\rho_p\frac{\partial u_p}{\partial t} = -\frac{\rho_p}{\tau_p}(u_p - u), \tag{9}$$

$$\rho_p c_s\frac{\partial T_p}{\partial t} = -\frac{\rho_p c_s}{\tau_T}(T_p - T), \tag{10}$$

where u and u_p are, respectively, the velocity of the fluid and of the particle phase.

The inner and outer cylinders are maintained at uniform temperatures T_a and T_b, respectively. The boundary conditions of the problem can be written as,

$$u = 0, \quad T = T_n \quad \text{at } r = a, \tag{11}$$

$$u = 0, \quad T = T_b \quad \text{at } r = b. \tag{12}$$

The flow is induced by a pulsatile pressure gradient of the form

$$-\frac{\partial p}{\partial z} = A\{1 + \epsilon\cos\omega t\}, \tag{13}$$

where ω is the frequency of the oscillation, A being a constant with a unit of pressure gradient and ϵ is a dimensionless small quantity.

Following Smith (1976) and Duck (1980), we can take $U = A(a-b)^2/\mu$ as a reference velocity and then the Reynolds number can be defined as $\mathrm{Re} = A(a-b)^3/\rho\nu^2$, ν being the kinematic viscosity of the fluid. We also introduce a frequency parameter $\beta_1 = \nu/a^2\omega$ (the square of the ratio of the Stokes layer thickness to the radius of the outer cylinder), and another parameter $\beta = \nu/(a-b)^2\omega = \beta_1/(1-\lambda)^2$.

The following dimensionless variables have been introduced to derive the dimensionless form of the above equations,

$$\xi = \frac{z}{a-b}, \qquad p^* = \frac{p}{A(a-b)}, \qquad \theta = \frac{T - T_b}{T_a - T_b},$$

$$\eta = \frac{r}{a-b}, \qquad u^* = \frac{u}{U}, \qquad \theta_p = \frac{T_p - T_b}{T_a - T_b}.$$

$$t^* = t\omega, \qquad u_p^* = \frac{u_p}{U},$$

The non-dimensional forms of [7]–[10] can be written as (for convenience the asterisks have been dropped),

$$(1-\phi)\frac{\partial u}{\partial t} = -\beta\frac{\partial p}{\partial \xi} + \beta\left\{\frac{\partial^2 u}{\partial \eta^2} + \frac{1}{\eta}\frac{\partial u}{\partial \eta}\right\} + f\alpha(u_p - u), \tag{14}$$

$$(1-\phi)\frac{\partial \theta}{\partial t} = \frac{\beta}{\mathrm{Pr}}\left\{\frac{\partial^2 \theta}{\partial \eta^2} + \frac{1}{\eta}\frac{\partial \theta}{\partial \eta}\right\} + \beta\,\mathrm{Ec}\left(\frac{\partial u}{\partial \eta}\right)^2 + f\alpha\,\mathrm{Ec}(u_p - u)^2 + \frac{2}{3}\frac{f\alpha}{\mathrm{Pr}}(\theta_p - \theta), \tag{15}$$

$$\frac{\partial u_p}{\partial t} = -\alpha(u_p - u), \tag{16}$$

$$\frac{\partial \theta_p}{\partial t} = -\frac{2}{3}\frac{\alpha}{\mathrm{Pr}\,\gamma}(\theta_p - \theta). \tag{17}$$

The parameters appearing in the above equations are

$$\mathrm{Pr} = \frac{\mu c_p}{k}, \qquad f = \frac{\rho_p}{\rho},$$

$$\lambda = \frac{b}{a}, \qquad \alpha = \frac{1}{\omega\tau_p}, \qquad \mathrm{Ec} = \frac{U^2}{c_p(T_a - T_b)}.$$

$$\tau_p = \frac{2}{3\,\mathrm{Pr}\,\gamma}\tau_T, \qquad \gamma = \frac{c_s}{c_p},$$

Here Pr, α, λ, Ec and f are the Prandtl number, dust parameter, aspect ratio, Eckert number and mass concentration of the dust particles, respectively.

The corresponding dimensionless boundary conditions are

$$\left.\begin{aligned} u = 0, \quad \theta = 0 \quad \text{at } \eta = \eta_b, \\ u = 0, \quad \theta = 1 \quad \text{at } \eta = \eta_a, \end{aligned}\right\} \tag{18}$$

where

$$\eta_a = \frac{1}{1-\lambda} \quad \text{and} \quad \eta_b = \frac{\lambda}{1-\lambda}.$$

The non-dimensional form of [13] will be

$$-\frac{\partial p}{\partial \xi} = 1 + \epsilon\cos t \tag{19}$$

3. METHOD OF SOLUTION

For convenience of solving the problem we introduce complex variables so that real parts will represent the physical entities. Thus [19] is rewritten as,

$$-\frac{\partial p}{\partial \xi} = 1 + \epsilon e^{it}, \tag{20}$$

i being the complex number $\sqrt{-1}$.

Then the solution of u, u_p, θ and θ_p can be assumed in the form,

$$\left.\begin{aligned} u(\eta, t) &= u_0(\eta) + \epsilon u_1(\eta)e^{it} \\ u_p(\eta, t) &= u_{p0}(\eta) + \epsilon u_{p1}(\eta)e^{it} \end{aligned}\right\} \tag{21}$$

$$\left.\begin{aligned} \theta(\eta, t) &= \theta_0(\eta) + \epsilon\theta_1(\eta)e^{it} + \epsilon^2\theta_2(\eta)e^{2it} \\ \theta_p(\eta, t) &= \theta_{p0}(\eta) + \epsilon\theta_{p1}(\eta)e^{it} + \epsilon^2\theta_{p2}(\eta)e^{2it} \end{aligned}\right\}, \tag{22}$$

where subscript 0 indicates the steady part and 1 and 2 indicate the first and second unsteady parts of the entities.

Using [20]–[22] in [14]–[17] and equating separately the terms free from ϵe^{it}, the coefficient of ϵe^{it} and that of $\epsilon^2 e^{2it}$, we get the following three sets of equations:

First set: steady part

$$\frac{\beta}{\eta}\frac{\mathrm{d}}{\mathrm{d}\eta}\left(\eta\frac{\mathrm{d}u_0}{\mathrm{d}\eta}\right)+f\alpha(u_{p0}-u_0)+\beta=0 \tag{23}$$

$$\frac{\beta}{\mathrm{Pr}}\frac{1}{\eta}\frac{\mathrm{d}}{\mathrm{d}\eta}\left(\eta\frac{\mathrm{d}\theta_0}{\mathrm{d}\eta}\right)+\beta\,\mathrm{Ec}\left(\frac{\mathrm{d}u_0}{\mathrm{d}\eta}\right)^2+f\alpha\,\mathrm{Ec}(u_{p0}-u_0)^2+\frac{2}{3}\frac{f\alpha}{\mathrm{Pr}}(\theta_{p0}-\theta_0)=0 \tag{24}$$

$$\alpha(u_{p0}-u_0)=0 \tag{25}$$

$$\frac{2}{3}\frac{\alpha}{\mathrm{Pr}\,\gamma}(\theta_{p0}-\theta_0)=0 \tag{26}$$

Second set: first unsteady part

$$\frac{\beta}{\eta}\frac{\mathrm{d}}{\mathrm{d}\eta}\left(\eta\frac{\mathrm{d}u_1}{\mathrm{d}\eta}\right)+f\alpha(u_{p1}-u_1)-i(1-\phi)u_1+\beta=0 \tag{27}$$

$$\frac{\beta}{\mathrm{Pr}}\frac{1}{\eta}\frac{\mathrm{d}}{\mathrm{d}\eta}\left(\eta\frac{\mathrm{d}\theta_1}{\mathrm{d}\eta}\right)+2\beta\,\mathrm{Ec}\frac{\mathrm{d}u_0}{\mathrm{d}\eta}\frac{\mathrm{d}u_1}{\mathrm{d}\eta}+2\,\mathrm{Ec}\,f\alpha(u_{p0}-u_0)(u_{p1}-u_1)$$
$$+\frac{2f\alpha}{3\,\mathrm{Pr}}(\theta_{p1}-\theta_1)-i(1-\phi)\theta_1=0 \tag{28}$$

$$\alpha(u_{p1}-u_1)+iu_{p1}=0 \tag{29}$$

$$\frac{2}{3}\frac{\alpha}{\mathrm{Pr}\,\gamma}(\theta_{p1}-\theta_1)+i\theta_{p1}=0 \tag{30}$$

Third set: second unsteady part

$$\frac{\beta}{\mathrm{Pr}}\frac{1}{\eta}\frac{\mathrm{d}}{\mathrm{d}\eta}\left(\eta\frac{\mathrm{d}\theta_2}{\mathrm{d}\eta}\right)+\beta\,\mathrm{Ec}\left(\frac{\mathrm{d}u_1}{\mathrm{d}\eta}\right)^2+\mathrm{Ec}\,f\alpha(u_{p1}-u_1)^2+\frac{2}{3}\frac{f\alpha}{\mathrm{Pr}}(\theta_{p2}-\theta_2)-2i(1-\phi)\theta_2=0 \tag{31}$$

$$\frac{2}{3}\frac{\alpha}{\mathrm{Pr}\,\gamma}(\theta_{p2}-\theta_2)+2i\theta_{p2}=0 \tag{32}$$

The corresponding boundary conditions, from [18], are

$$\left.\begin{aligned}u_0=0,\quad \theta_0=1\quad &\text{at}\ \eta=\eta_a\\ u_0=0,\quad \theta_0=0\quad &\text{at}\ \eta=\eta_b\end{aligned}\right\} \tag{33}$$

$$\left.\begin{aligned}u_1=0,\quad \theta_1=0\quad &\text{at}\ \eta=\eta_a\\ u_1=0,\quad \theta_1=0\quad &\text{at}\ \eta=\eta_b\end{aligned}\right\} \tag{34}$$

$$\left.\begin{aligned}\theta_2=0\quad &\text{at}\ \eta=\eta_a\\ \theta_2=0\quad &\text{at}\ \eta=\eta_b\end{aligned}\right\} \tag{35}$$

The expressions for u_0 and u_{p0} can be obtained after solving [23] and [25] under appropriate boundary conditions from [33] as,

$$u_0=\frac{\eta_a^2-\eta^2}{4}+A_1\log\left(\frac{\eta}{\eta_a}\right), \tag{36}$$

$$u_{p0}=u_0 \tag{37}$$

where

$$A_1=-\frac{1+\lambda}{4\log\lambda}\eta_a,$$

It may be noted that for a fully developed flow, the steady part of the fluid velocity and the particle phase velocity are the same.

Eliminating u_{p1} from [27] and [29], the differential equation for u_1 can be written as,

$$\frac{d^2u_1}{d\eta^2}+\frac{1}{\eta}\frac{du_1}{d\eta}-(c_1+ic_2)u_1=-1, \qquad [38]$$

where

$$c_1=\frac{f\alpha}{\beta(1+\alpha^2)} \quad \text{and} \quad c_2=\frac{(1-\phi)}{\beta}+\alpha c_1.$$

The solution of the above equation, satisfying the boundary conditions from [34] can easily be obtained as,

$$u_1=A_2I_0\{(a_1+ib_1)\eta\}+B_2K_0\{(a_1+ib_1)\eta\}+\frac{1}{c_1+ic_2}, \qquad [39]$$

where

$$a_1+ib_1=\sqrt{c_1+ic_2},$$

$$A_2=\frac{K_0\{(a_1+ib_1)\eta_a\}-K_0\{(a_1+ib_1)\eta_a\}}{c_1+ic_2}\frac{1}{D_2},$$

$$B_2=\frac{I_0\{(a_1+ib_1)\eta_b\}-I_0\{(a_1+ib_1)\eta_a\}}{c_1+ic_2}\frac{1}{D_2},$$

$$D_2=I_0\{(a_1+ib_1)\eta_a\}K_0\{(a_1+ib_1)\eta_b\}-K_0\{(a_1+ib_1)\eta_a\}I_0\{(a_1+ib_1)\eta_b\},$$

and I_0 and K_0 are the zeroth order modified Bessel functions of the first and second kind, respectively.

From [29], we have,

$$u_{p1}=\frac{\alpha(a-i)}{1+\alpha^2}u_1. \qquad [40]$$

Solving [24] and [26] using the expression of u_0 from [36] and the boundary conditions from [33], we get the following expressions for θ_0 and θ_{p0}:

$$\theta_0=\mathrm{Ec\,Pr}\left[\frac{1}{64}(\eta_b^4-\eta^4)-\frac{A_1}{4}(\eta_b^2-\eta^2)+\frac{A_1^2}{2}\{(\log\eta_a)^2-(\log\eta)^2\}\right.$$
$$\left.-\left\{\frac{A_1}{16}(1+\lambda^2)\eta_a^2-A_1^2+\frac{A_1^2}{2}\log(\eta_a\eta_b)\right\}\log\left(\frac{\eta_b}{\eta}\right)\right]+\frac{\log(\eta_b/\eta)}{\log\lambda} \qquad [41]$$

and

$$\theta_{p0}=\theta_0. \qquad [42]$$

The steady parts of the temperatures of the fluid and particle phase are the same.

Using the expressions of u_0 and u_1 and eliminating θ_{p1}, [28] and [30] give,

$$\frac{d^2\theta_1}{d\eta^2}+\frac{1}{\eta}\frac{d\theta_1}{d\eta}-(c_3+ic_4)\theta_1=F_1(\eta), \qquad [43]$$

where

$$c_3=\frac{6\,\mathrm{Pr}^2f\alpha\gamma^2}{\beta(4\alpha^2+9\,\mathrm{Pr}^2\gamma^2)}, \quad c_4=\frac{\mathrm{Pr}}{\beta}\left[\frac{4f\alpha^2\gamma}{4\alpha^2+9\,\mathrm{Pr}^2\gamma^2}+1-\phi\right],$$

and

$$F_1(\eta)=2\,\mathrm{Pr\,Ec}(a_1+ib_1)\left(\frac{A_1}{\eta}-\frac{\eta}{2}\right)[A_2I_0'\{(a_1+ib_1)\eta\}+B_2K_0'\{(a_1+ib_1)\eta\}],$$

prime denoting the derivative with respect to the argument.

Applying the method of the variation of parameters, we get the solution of [43] satisfying the boundary conditions [34] as,

$$\theta_1(\eta) = \theta_{12}(\eta) \int_{\eta_b}^{\eta} \frac{\theta_{11}(\eta)F_1(\eta)}{W_1(\eta)}\,d\eta + \theta_{11}(\eta) \int_{\eta}^{\eta_a} \frac{\theta_{12}(\eta)F_1(\eta)}{W_1(\eta)}\,d\eta, \quad [44]$$

where

$$\theta_{11}(\eta) = I_0\{(a_2 + ib_2)\eta\}K_0\{(a_2 + ib_2)\eta_b\} - K_0\{(a_2 + ib_2)\eta\}I_0\{(a_2 + ib_2)\eta_b\},$$

$$\theta_{12}(\eta) = I_0\{(a_2 + ib_2)\eta\}K_0\{(a_2 + ib_2)\eta_a\} - K_0\{(a_2 + ib_2)\eta\}I_0\{(a_2 + ib_2)\eta_a\},$$

$W_1(\eta) = W[\theta_{11}, \theta_{12}; \eta]$, the Wronskian of $\theta_{11}(\eta)$ and $\theta_{12}(\eta)$,

$$a_2 + ib_2 = \sqrt{c_3 + ic_4}.$$

From [30] we have

$$\theta_{p1} = \frac{2\alpha(2\alpha - 3i\,\mathrm{Pr}\,\gamma)}{4\alpha^2 + 9\,\mathrm{Pr}^2\gamma^2}\theta_1 \quad [45]$$

From [31] and [32], the differential equation for θ_2 can be written as,

$$\frac{d^2\theta_2}{d\eta^2} + \frac{1}{\eta}\frac{d\theta_2}{d\eta} - (c_5 + ic_6)\theta_2 = F_2(\eta), \quad [46]$$

where

$$c_5 = \frac{6\,\mathrm{Pr}^2 f\alpha\gamma^2}{\beta(\alpha^2 + 9\,\mathrm{Pr}^2\gamma^2)}, \quad c_6 = \frac{2\,\mathrm{Pr}}{\beta}\left\{\frac{f\alpha^2\gamma}{\alpha^2 + 9\,\mathrm{Pr}^2\gamma^2} + 1 - \phi\right\},$$

and

$$F_2(\eta) = -\mathrm{Pr}\,\mathrm{Ec}\left\{\frac{f\alpha(1 - \alpha^2 + 2i\alpha)}{\beta(1 + \alpha^2)^2}u_1^2 + \left(\frac{du_1}{d\eta}\right)^2\right\}.$$

Using the boundary conditions [35], the solution of [46] is,

$$\theta_2(\eta) = \theta_{22}(\eta) \int_{\eta_b}^{\eta} \frac{\theta_{21}(\eta)F_2(\eta)}{W_2(\eta)}\,d\eta + \theta_{21}(\eta) \int_{\eta}^{\eta_a} \frac{\theta_{22}(\eta)F_2(\eta)}{W_2(\eta)}\,d\eta, \quad [47]$$

where

$$\theta_{21}(\eta) = I_0\{(a_3 + ib_3)\eta\}K_0\{(a_3 + ib_3)\eta_b\} - K_0\{(a_3 + ib_3)\eta\}I_0\{(a_3 + ib_3)\eta_b\},$$

$$\theta_{22}(r) = I_0\{(a_3 + ib_3)\eta\}K_0\{(a_3 + ib_3)\eta_a\} - K_0\{(a_3 + ib_3)\eta\}I_0\{(a_3 + ib_3)\eta_a\},$$

$W_2(\eta) = W[\theta_{21}, \theta_{22}; \eta]$, the Wronskian of $\theta_{21}(\eta)$ and $\theta_{22}(\eta)$,

$$a_3 + ib_3 = \sqrt{c_5 + ic_6}.$$

From [32] we have

$$\theta_{p2} = \frac{\alpha(\alpha - 3i\,\mathrm{Pr}\,\gamma)}{\alpha^2 + 9\,\mathrm{Pr}^2\gamma^2}\theta_2. \quad [48]$$

4. DISCUSSION OF RESULTS

In order to discuss results, figures 2–10 have been presented for some representative values of the parameters. We have taken $\rho_s/\rho = 10$, $\mathrm{Pr} = 0.72$, $\mathrm{Ec} = 0.02$, $\gamma = 1.4$, $\alpha = 1.0$ and $\epsilon = 0.1$. In order to consider the effect of the frequency parameter β_1, we have taken $\beta_1 = 0.0625$, 0.25 and 2.25.

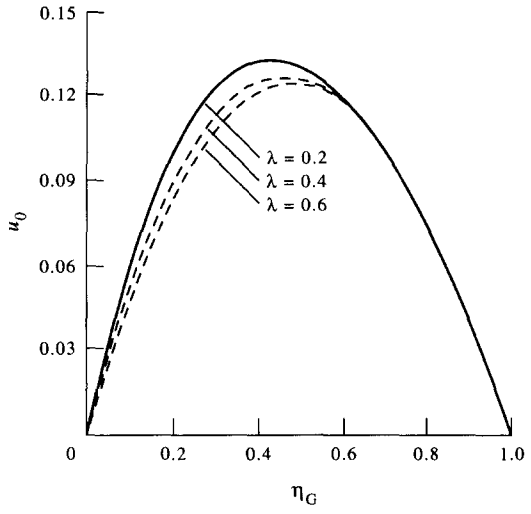

Figure 2. Variation of the steady part of the velocity against η_G.

Similarly, for finding the effect of the volume fraction of the particles we have taken $\phi = 0.0$ to 0.05, since for $\phi > 0.055$, the particle–particle interaction is not negligible (Soo 1976). Also, to get the variation of results with change in aspect ratio of the annular pipe we have considered $\lambda = 0.1$ to 0.9. All the calculations, including the values of the modified Bessel functions I_0 and K_0 and the integrations in [44] and [47], have been performed numerically. The graphs are presented against a new independent variable $\eta_G = \eta - \eta_b$, for convenience.

Figure 2 shows the profiles of the steady part of the fluid velocity for various values of λ. It is observed that the steady velocity decreases with increase of λ, i.e. decrease of annular gap. Further, the profiles are nearly parabolic and from [37] it is seen that the steady part of the fluid velocity is equal to that of the particle phase velocity.

Figure 3(a) and (b) represents the profiles of the amplitude of the unsteady part of the velocity of the fluid as well as that of the particle phase for different values of β_1 and λ, respectively. It is observed that the amplitude increases with increase of λ and also with increase of β_1 for both phases. Physically, β_1 increases with decrease of frequency of oscillation ω, which in turn would increase the pressure gradient resulting in an increase of velocity. The unsteady velocity of the particle phase is always less than that of the fluid.

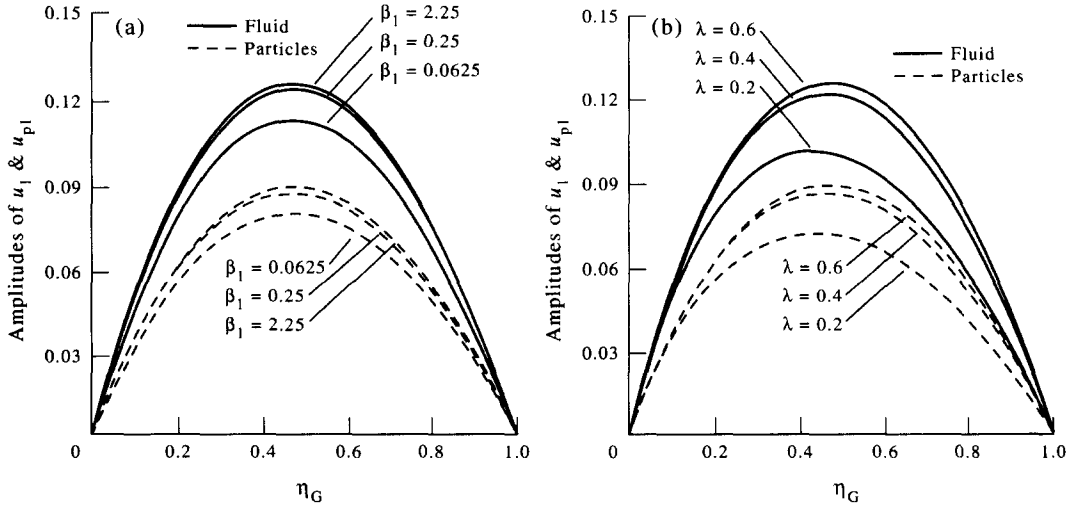

Figure 3. (a) Variation of the amplitude of the unsteady velocity against η_G when $\lambda = 0.5$ and $\phi = 0.02$.
(b) Variation of the amplitude of the unsteady velocity against η_G when $\beta_1 = 0.5$ and $\phi = 0.02$.

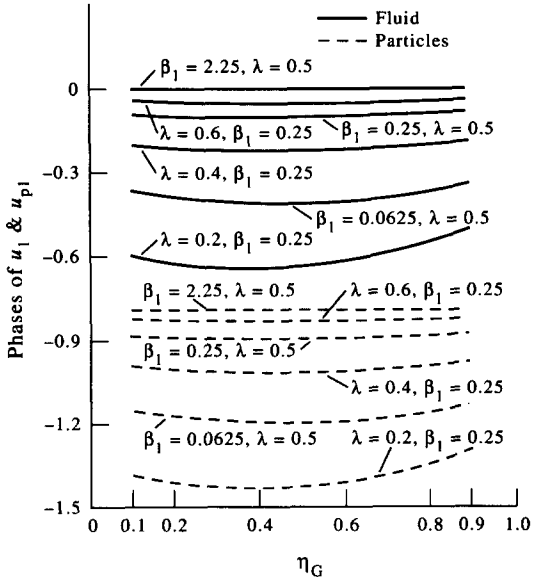

Figure 4. Variation of the phase of the unsteady velocity against η_G when $\phi = 0.02$.

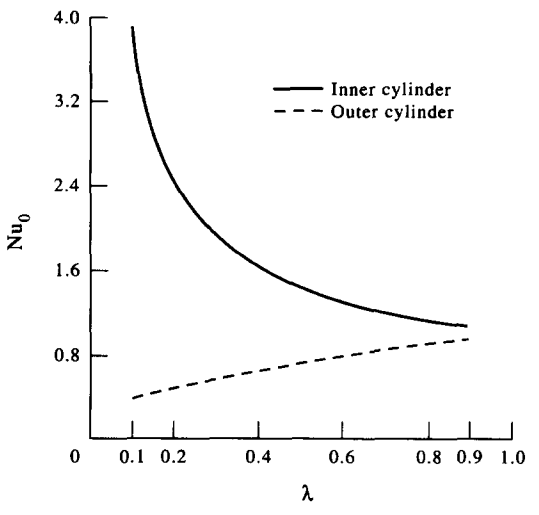

Figure 5. Variation of the steady Nusselt number against λ.

The profiles of the phase lag of the unsteady part of the velocities of the fluid and of the particle phase for different λ and β_1 have been drawn in figure 4. It is seen that the phase lag decreases with increase of λ as well as with increase of β_1 for both phases, and the phase lag of the particle phase is more than that of the fluid.

In order to discuss the heat transfer at the walls we consider the Nusselt number (Nu) of the fluid at the walls given by

$$\begin{aligned} \mathrm{Nu} &= -\left.\frac{\partial\theta}{\partial\eta}\right|_{\text{at } \eta=\eta_a \text{ or } \eta=\eta_b} \\ &= -\left[\frac{\mathrm{d}\theta_0}{\mathrm{d}\eta} + \epsilon e^{it}\frac{\mathrm{d}\theta_1}{\mathrm{d}\eta} + \epsilon^2 e^{2it}\frac{\mathrm{d}\theta_2}{\mathrm{d}\eta}\right]_{\text{at } \eta=\eta_a \text{ or } \eta=\eta_b} \\ &= -[\mathrm{Nu}_0 + \epsilon e^{it}\,\mathrm{Nu}_1 + \epsilon^2 e^{2it}\,\mathrm{Nu}_2]_{\text{at } \eta=\eta_a \text{ or } \eta=\eta_b}, \end{aligned} \qquad [49]$$

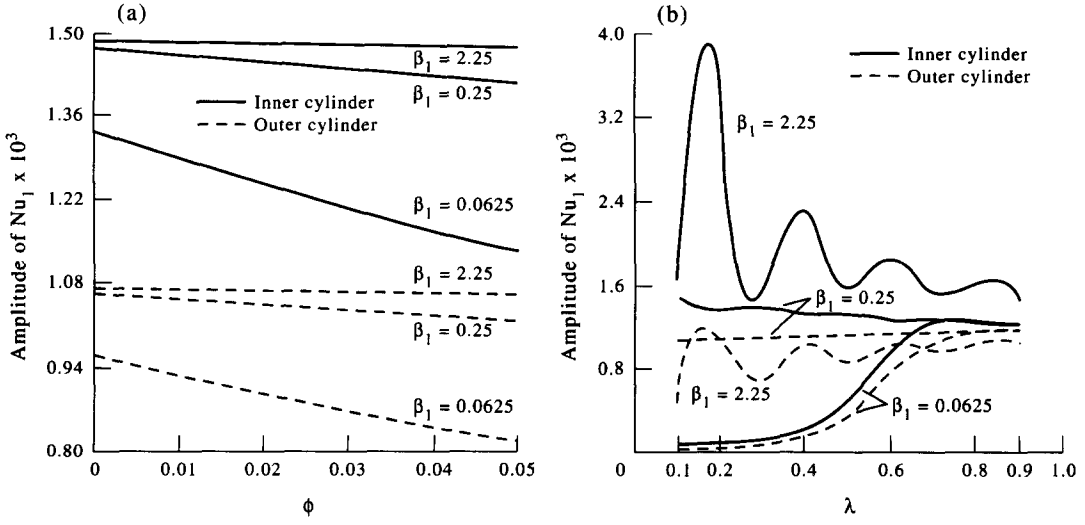

Figure 6. (a) Variation of the amplitude of the first unsteady part of the Nusselt number against ϕ when $\lambda = 0.5$. (b) Variation of the amplitude of the first unsteady part of the Nusselt number against λ when $\phi = 0.02$.

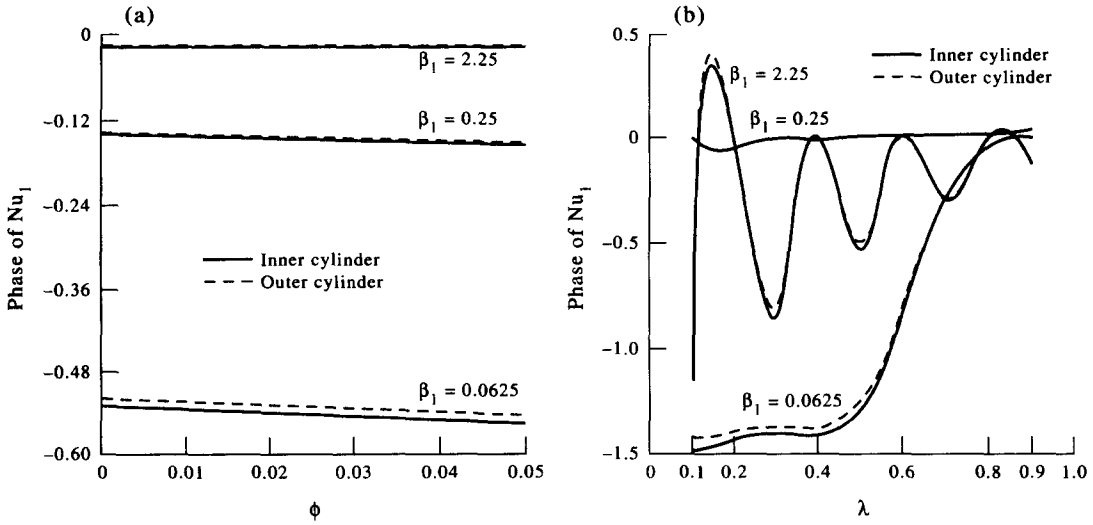

Figure 7. (a) Variation of the phase of the first unsteady part of the Nusselt number against ϕ when $\lambda = 0.5$. (b) Variation of the phase of the first unsteady part of the Nusselt number against λ when $\phi = 0.02$.

where terms Nu_0, Nu_1 and Nu_2 correspond to the steady part, the first unsteady part and the second unsteady part of the Nusselt number, respectively, and are given by

$$Nu_0|_{\eta=\eta_a} = Ec\,Pr\left[\frac{\eta_a^3}{16} - \frac{A_1\eta_a}{2} + \frac{A_1^2}{\eta_a}\log\eta_a\right] - \frac{B_1}{\eta_a}, \quad [50]$$

$$Nu_0|_{\eta=\eta_b} = Ec\,Pr\left[\frac{\eta_b^3}{16} - \frac{A_1\eta_b}{2} + \frac{A_1^2}{\eta_b}\log\eta_b\right] - \frac{B_1}{\eta_b}, \quad [51]$$

$$Nu_1|_{\eta=\eta_a} = -\left.\frac{d\theta_{12}}{d\eta}\right|_{\eta=\eta_a} \int_{\eta_b}^{\eta_a} \frac{\theta_{11}(\eta)F_1(\eta)}{W_1(\eta)}\,d\eta, \quad [52]$$

$$Nu_1|_{\eta=\eta_b} = -\left.\frac{d\theta_{11}}{d\eta}\right|_{\eta=\eta_b} \int_{\eta_b}^{\eta_a} \frac{\theta_{12}(\eta)F_1(\eta)}{W_1(\eta)}\,d\eta, \quad [53]$$

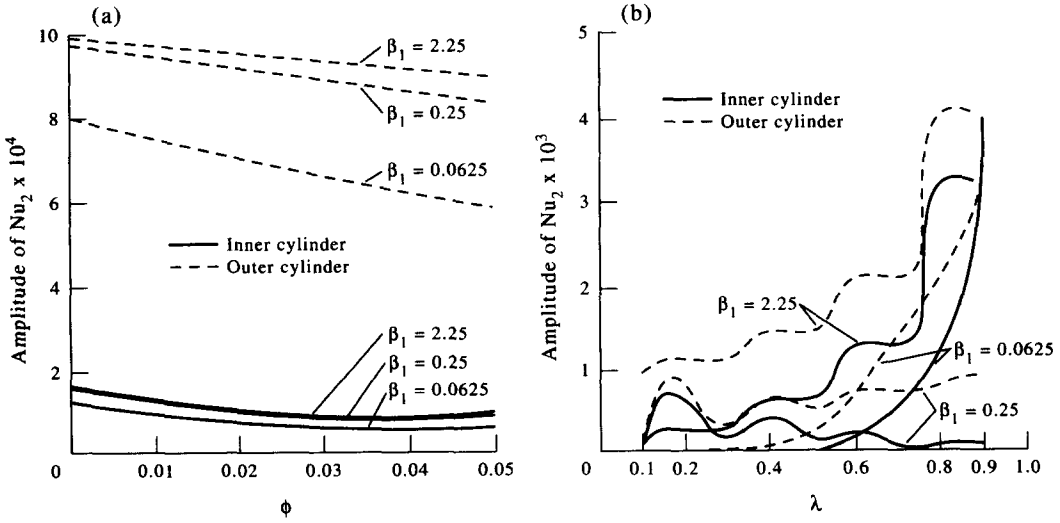

Figure 8. (a) Variation of the amplitude of the second unsteady part of the Nusselt number against ϕ when $\lambda = 0.5$. (b) Variation of the amplitude of the second unsteady part of the Nusselt number against λ when $\phi = 0.02$.

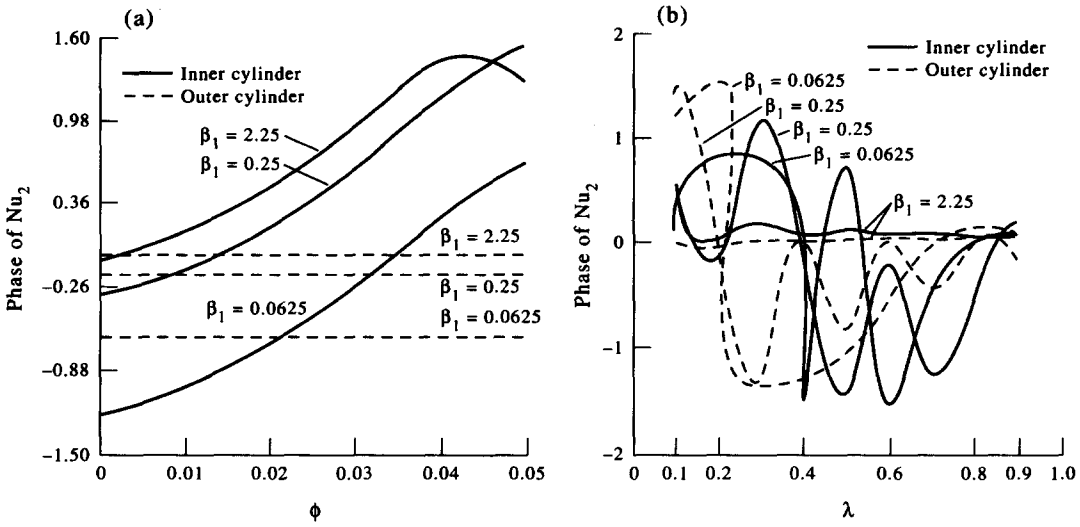

Figure 9. (a) Variation of the phase of the second unsteady part of the Nusselt number against ϕ when $\lambda = 0.5$. (b) Variation of the phase of the second unsteady part of the Nusselt number against λ when $\phi = 0.02$.

$$\mathrm{Nu}_2|_{\eta=\eta_a} = -\frac{\mathrm{d}\theta_{22}}{\mathrm{d}\eta}\bigg|_{\eta=\eta_a} \int_{\eta_b}^{\eta_a} \frac{\theta_{21}(\eta)F_2(\eta)}{W_2(\eta)}\,\mathrm{d}\eta, \qquad [54]$$

$$\mathrm{Nu}_2|_{\eta=\eta_b} = -\frac{\mathrm{d}\theta_{21}}{\mathrm{d}\eta}\bigg|_{\eta=\eta_b} \int_{\eta_b}^{\eta_a} \frac{\theta_{22}(\eta)F_2(\eta)}{W_2(\eta)}\,\mathrm{d}\eta, \qquad [55]$$

and

$$B_1 = \mathrm{Ec}\,\mathrm{Pr}\left[\frac{A_1(1+\lambda^2)\eta_a^2}{16} + \frac{A_1^2}{2}\log(\eta_a\eta_b) - A_1^2\right] - \frac{1}{\log\lambda}.$$

The graph of the steady part of the Nusselt number against λ is shown in figure 5. It is seen that at the inner cylinder, this decreases with increase of the aspect ratio λ, but at the outer cylinder the effect is opposite. The rate of heat transfer at the outer cylinder is less than that at the inner cylinder.

The variation of amplitude of the first unsteady part of the Nusselt number against volume fraction ϕ for different values of β_1 is shown in figure 6(a) and that against λ in figure 6(b). It is

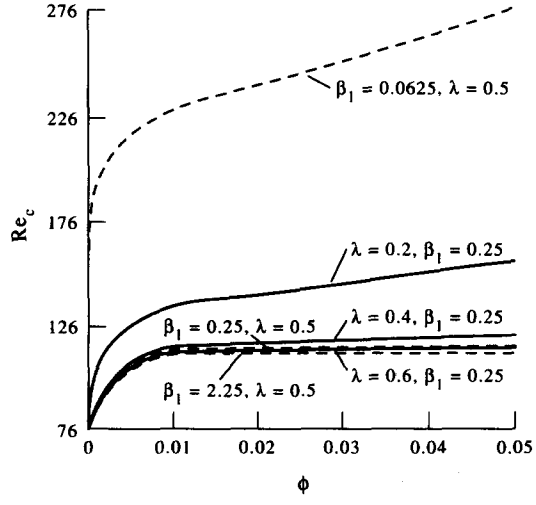

Figure 10. Variation of critical Reynolds number against ϕ.

observed that the amplitude increases with increase of β_1 and decreases with increase of ϕ. For small β_1, i.e. for a high frequency of oscillation, the variation in heat transfer with ϕ is significant whereas for large β_1 this effect is almost constant. The nature of the variation of the rate of heat transfer against λ at the outer cylinder is similar than that at the inner cylinder. However, the rate of heat transfer at the outer cylinder is less than that at the inner cylinder. For large β_1, the variation of heat transfer rate with λ is oscillatory, however, these oscillations diminish as λ increases (i.e. annular gap decreases).

Figure 7(a) and (b) shows the variation of the phase lag of the first unsteady part of the Nusselt number of the fluid at the outer and at the inner cylinder for different values of β_1, ϕ and λ. We observe that the phase lag increases slowly with ioncrease of ϕ but it decreases with increase of β_1. The phase lag at the inner cylinder is more than that at the outer cylinder but the difference in the phase lag at the inner and at the outer cylinder decreases with increase of β_1. Phase lag decreases with increase of λ for small β_1, i.e. for a large frequency of oscillation in a pressure gradient, but with an increase of β_1 the variation in phase lag with λ becomes small and for large β_1 (i.e. when the frequency of oscillation is small), there is a damped oscillation in the phase lag with an increase of λ.

The variation of the amplitude of the second unsteady part of the Nusselt number at the inner and at the outer cylinder with ϕ, β_1 and λ has been shown in figure 8(a) and (b). It is seen that the amplitude of the second unsteady part of the Nusselt number increases with increase of β_1 at both cylinders and decreases with increase of ϕ at the outer cylinder, whereas at the inner cylinder it decreases with increase of ϕ upto a certain value and after that it increases with an increase of ϕ. The amplitude of Nu_2 at the inner cylinder as well as that at the outer cylinder increases with increase of aspect ratio λ.

Figure 9(a) exhibits the graphs of the phase difference of the second unsteady part of the Nusselt number at the inner and at the outer cylinder against ϕ for different values of β_1 and figure 9(b) shows the same against λ. It can be seen that the phase difference of the second unsteady part of the Nusselt number at the inner cylinder changes from phase lag to phase lead with increase of ϕ, but at the outer cylinder it is always a phase lag. With increase of λ, the variation of phase difference is oscillatory and the amplitude of this oscillation decreases with increase of either β_1 or λ.

In the present modelling we have assumed that the Reynolds number based on the relative velocity of the particle phase has to be less than 1.0. So we can write.

$$\frac{|u_p - u|(a-b)}{\nu} < 1.0.$$

Using the dimensionless variables u^*, u_p^* and parameter Re, the above inequality can be written as (dropping the superscripts),

$$\mathrm{Re} < \frac{1}{\epsilon} |u_{p1} - u_1|.$$

Now,

$$\mathrm{Re}_c = \frac{1}{\epsilon} |u_{p1} - u_1|,$$

Re_c is called the critical Reynolds number of the fluid, i.e. the Reynolds number of the fluid has to be less than Re_c so as to satisfy our assumptions.

Figure 10 shows the graph of critical Reynolds number against ϕ for different values of β_1 and λ. It is seen that the critical Reynolds number Re_c increases slowly with increase of ϕ and decreases with increase of either β_1 or λ.

5. CONCLUSIONS

From the theoretical investigation of the pulsatile flow and heat transfer of a dusty fluid through the annulus of two concentric pipes the following observations can be made.

The steady parts of the flow of the fluid and the particle phase are the same and they decrease with decrease of the annular gap; whereas the amplitudes of the unsteady velocity of the fluid and of the particle phase increase with decrease of this gap. The steady parts of the velocity are large compared to the amplitude of the unsteady parts. The combined velocity of the fluid, as well as of the particle phase, decreases with decrease of the gap between the cylinders. This occurs due to the effect of the viscosity of the fluid near the walls of the annulus. With a decrease of the annular gap the steady part of the rate of heat transfer increases at the outer wall whereas that at the inner wall decreases. The amplitude of the unsteady part of the rate of heat transfer is much smaller than the steady one and oscillates with a decrease of the annular gap.

The amplitudes of the unsteady parts of the rate of heat transfer at both walls decrease with an increase of the frequency of oscillation of the pulsating pressure gradient.

The effect of the increase of volume fraction on the heat transfer rate at both walls is to decrease it for a large frequency of oscillation.

*Acknowledgement*s—One of us (D. C. Dalal) wishes to express his thanks to CSIR (India) for granting a fellowship to pursue this work. We are grateful to the reviewers whose suggestions have helped us to improve this paper in this revised version.

REFERENCES

DEPEW, C. A. & KRAMER, T. J. 1973 Heat transfer to flowing gas–solid mixtures. *Advances in Heat Transfer*, Vol. 9. Academic Press, New York.

DUCK, P. W. 1980 Pulsatile flow through constricted and dilated channels. *Q. Jl Mech. Appl. Math.* **33,** 77–92.

HAN, K. S., SUNG, H. J. & CHUNG, M. K. 1991 Analysis of heat transfer in a pipe carrying two-phase gas-particle suspension. *Int. J. Heat Mass Transfer* **34,** 69–78.

HEATON, H. S., REYNOLDS, W. C. & KAYS, W. M. 1962 Heat transfer with laminar flow in concentric annuli with constant heat flux and simultaneously developing velocity and temperature distributions. Stanford University, CA.

JAKOB, M. & REES, K. 1941 Heat transfer to a fluid in laminar flow through an annular space. *Trans. AIChE* **37,** 619–648.

LEUNG, E. Y., KAYS, W. M. & REYNOLDS, W. C. 1962 Heat transfer with turbulent flow in concentric and eccentric annuli with constant and variable heat flux. Report No. AHT-4, Stanford University, CA.

MARBLE, F. E. 1962 Dynamics of a gas containing small solid particles. In Braunschweig *Proceedings of the 5th AGARD Combustion and Propulsion Colloquium*, pp. 175–215. Pergamon Press, Oxford (1963).

MCCUEN, P. A., KAYS, W. M. & REYNOLDS, W. C. 1961 Heat transfer with laminar flow in concentric annuli with constant and variable wall temperature and heat flux. Report No. AHT-2, Stanford University, CA.

MCCUEN, P. A., KAYS, W. M. & REYNOLDS, W. C. 1962 Heat transfer with laminar flow and turbulent flow between parallel planes with constant and variable wall temperature and heat flux. Report No. AHT-3, Stanford University, CA.

MICHAELIDES, E. E. 1986 Heat transfer in particulate flows. *Int. J. Heat Mass Transfer* **29,** 265–273.

REYNOLDS, W. C., MCCUEN, P. A., LUNDBERG, R. E., LEUNG, Y. W., & HEATON, H. S. 1960 Heat transfer in annular passages with variable wall temperature and heat flux. Report No. AHT-1, Stanford University, CA.

REYNOLDS, W. C., LUNDBERG, R. E. & MCCUEN, P. A. 1963 Heat transfer in annular passages. General formulation of the problem for arbitrarily prescribed wall temperatures and heat fluxes. *Int. J. Heat Mass Transfer* **6,** 483–493.

SAFFMAN, P. G. 1962 On the stability of laminar flow of a dusty gas. *J. Fluid Mech.* **13,** 120–128.

SHIGECHI, T. & LEE, Y. 1991 An analysis on fully developed laminar flow and heat transfer in concentric annuli with moving cores. *Int. J. Heat Mass Transfer* **34,** 2593–2601.

SINGH, D. 1973 Flow of a dusty gas through the annular space between two concentric circular cylinders. *Indian J. Phys.* **47,** 341–346.

SINGLETON, R. E. 1965 The compressible gas–solid particle flow over a semi-infinite flat plate. *ZAMP* **16,** 421–449.

SMITH, F. T. 1976 Flow through constricted or dilated pipes and channels. *Q. Jl Mech. Appl. Math.* **29,** 343–364.

SOO, S. L. 1976 Net effect of pressure gradient on a sphere. *Phys. Fluids* **19,** 757.

SOUNDALGAKAR, V. M., BHAT, J. P. & GUPTA, A. S. 1989 Heat transfer in a pulsatile flow of an elastico-viscous fluid in a porous plate channel. *Model. Sim. Control B* **31,** 1–22.

UCHIDA, S. 1956 The pulsating viscous flow superposed on the steady laminar motion of incompressible fluid in a circular pipe. *ZAMP* **7,** 403–422.